JOURNAL OF MAGNETIC RESONANCE **127,** 233–237 (1997)
ARTICLE NO. MN971200

Compact MRI Magnet Design by Stochastic Optimization

Stuart Crozier* and David M. Doddrell

Centre for Magnetic Resonance, The University of Queensland, St. Lucia, Queensland 4072, Australia

Received February 5, 1997

In this Communication, we describe a stochastic method of MRI magnet design that produces viable designs for actively shielded, whole-body MRI magnets of total coil length less than 1.3 m. The advantages of making the magnet as short as possible include the potential to reduce the perception of claustrophobia for the patient, better access by attending physicians, and reduced costs of siting a small system. Conventional medical MRI systems are typically around 1.8–2.0 m in length with free bore diameters in the range of 0.8–1.0 (*1–7*).

A major challenge in designing a short magnet is the retention of high homogeneity conditions over the diameter sensitive volume (dsv), as magnet homogeneity is strongly dependent on the overall length of the coil structure. A bare magnet homogeneity requirement of 20 ppm or less over the dsv is common for MRI systems. It is also important that the spatial distribution of the inhomogeneity in the field be characterized by low order terms after construction, so that they may be removed by passive or active (superconducting) shimming. The theoretical design process, therefore, must place special emphasis on reducing the higher order terms. Due to the necessary symmetry in the magnets, only even order zonal harmonics of the field expansion need be considered (*1, 2*).

Many of the early magnet designs, in terms of coil structure, were based on the seminal work of Garrett (*1, 2*). In this work, simple recurrence relationships were presented for the direct calculation of field spherical harmonics from coil bundles of arbitrary (rectilinear) cross-sections and current densities. Furthermore, the design of a range of magnets was detailed so that zonal harmonic impurities up to a designated order were nulled. To null all harmonic impurities out to 12th order, for example, a six-coil magnet was needed (2). In order to reduce stray fields from a magnet and thus provide siting and safety benefits, active and passive shielding have been used in magnet structures over the last decade or so (*3–6*).

* To whom correspondence should be addressed.

Our goal in this work was to design an actively shielded magnet, while restricting the overall length of the coil in a magnet to less than 1.25 m with a free bore of 0.9 m, subject to the constraints of the homogeneity being <20 ppm peak-to-peak over a 45-cm dsv and the fringe field being minimized, that is, the 0.5 mT (5 G) contour being as close to the magnet as is practicable.

We (*8–10*) and others (*11*) have shown that the simulated annealing method (SA) (*12*) is effective for compact gradient design and so now apply this method to magnet design. SA has been successfully applied to other electromagnetic design problems (e.g., *13–15*). By imposing length constraints, the SA routine effectively attempts to find the best solution possible within these limits. Here ''best'' refers to the minimization of an error function which, in this case, contains terms representing the homogeneity of the dsv and the quality of shielding. It is possible to include other terms in the function as the designer requires. The error function for the designs presented here was

$$E = k_a \sum_{n=1}^{9} k_n A_{2n} + k_b \left(\sum_{m=1}^{l} B_{\mathrm{mod}}(z_m) + \sum_{m=1}^{l} B_{\mathrm{mod}}(y_m) \right), \quad [1]$$

where k_a and k_b are the weighting factors for the homogeneity and shielding terms, respectively, k_n are the weighting factors for the zonal harmonics, and A_{2n} are the amplitudes of the even order zonal harmonics of B_z. The two summations of the shielding term are respectively longitudinal and vertical field additions at the chosen shielding distances, and for each iteration 10 points per direction were summed (i.e., $l = 10$).

The homogeneity term is the most difficult to minimize and so was weighted 5:1 when compared to the shielding term. Even order zonal harmonics were weighted 1:10:100:1000:5000:5000:5000:5000:5000 up to 18th order. A disadvantage of the SA procedure is that it takes many iterations to achieve its ''frozen'' state (*12*) and it is therefore important that the time for each iteration be as short as possible. Fortunately, the method for direct

1090-7807/97 $25.00

field harmonic calculation presented by Garrett (*1*) is rapid, calculating harmonics up to 18th order from a 14-coil magnet in under 100 ms on a SUN SPARCstation 10. A calculation of the field in the dsv by elliptical integral calculations (16) for all turns in a typical magnet takes more than 2 min on the same computer. To calculate the field for shielding and for checking the peak-to-peak and rms field variations over the dsv, we have developed a rapid field calculation routine based on the coil cross-section (that is, the computation time is independent of the number of turns) (*17*) which is in essence a modified version of the methods presented by Urankur (*18*) and Babic *et al.* (*19*). The total time per iteration to evaluate the error function in [1] for each magnet configuration was less than 300 ms for all designs presented here, thus permitting the thousands of iterations necessary for stochastic optimization to be performed in reasonable times.

The parameters for perturbation in the design process for each coil were the axial and radial dimensions of the coil, the number of turns per coil and the radial and axial position of each coil. In order to introduce sufficient degrees of freedom in these constrained problems, we begin with relatively large numbers of coils (16 primary coils, 4 shielding coils) and allow the SA process to redistribute them. Adaptive step sizing (20) was implemented and initial step sizes and temperatures selected by testing each coil for parametric sensitivity prior to the SA run. Each magnet design took 4–6 h to compete and consisted of 2 SA runs, the first having coarse steps and was limited to one hour, after which overlapping coils were coalesced and the algorithm restarted. Figure 1 shows the error path of these two runs; note the positive error excursions typical of SA and the slow progression to the better minima.

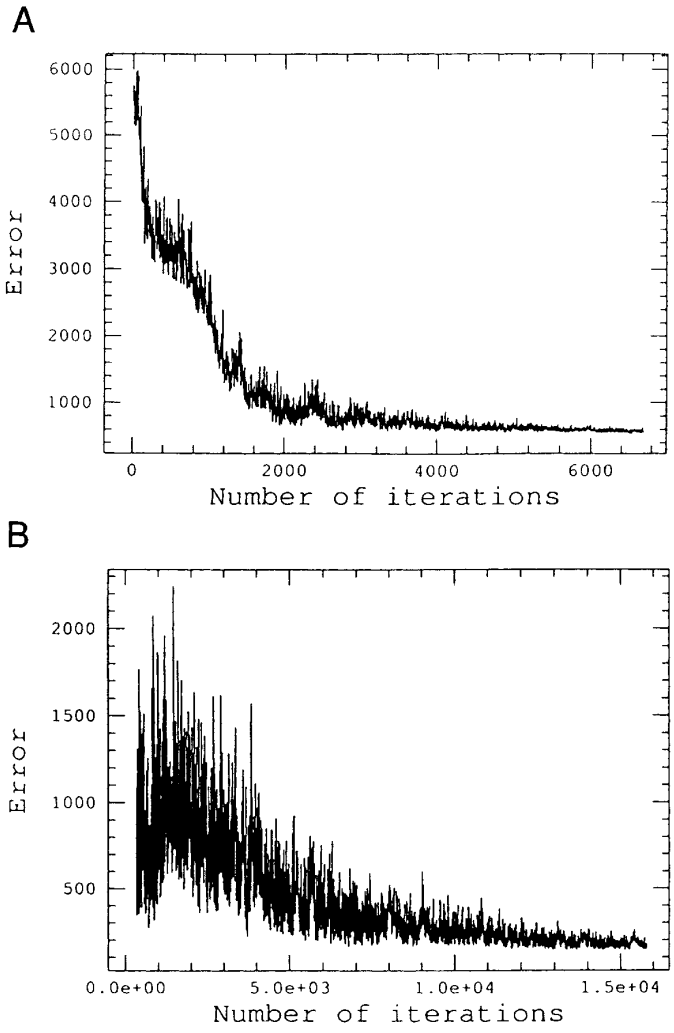

FIG. 1. The error paths of a typical optimization run in two parts: (A) coarse first run of limited iterations and (B) final run after overlapping coil coalescence.

Figure 2 shows the schematic of the resultant compact design in cross-section and its relation to the dsv. Figure 3 shows an expanded view of one quadrant of this design, coils marked with a negative sign are counter wound to the others. Figure 4 shows an alternative design using coils with smaller turns density (larger cross-section wire). These designs differ markedly from conventional six-coil magnets (21), in six-coil designs all primary coils are typically wound in the same direction (let us say has all positive windings). As the length constraints were introduced, the SA algorithm repeatedly allocated some coils in the primary magnet with negative turns to achieve the desired homogeneity. This appears to be a mechanism for shortening magnet design when all primary coils are on essentially the same diameter. The disadvantage, of course, is that more turns are required to achieve a designated field strength (1 T in these cases) than are required without negative turns in the primary coils.

The performance results of these two designs are given in Table 1 and indicate high homogeneity and shielding quality. The harmonics of the field were calculated to 18th order and the peak-to-peak and rms field deviations were calculated over 360 points on the surface of the dsv in 12 planes, the distribution of these planes being chosen to be the zeros of the 12th order Legendre polynomial so that Gaussian integration may be readily implemented (*22*). We have verified the accuracy of our field and harmonic calculations by comparison with commercial electromagnetics software (Vector Fields, Oxford); the results were within 3 ppm of each other. Note that the homogeneity figures are bare homogeneity values (i.e., no shimming). Shielding calculations for the final designs were made at 100 points along longitudinal and vertical axes at the desired radial and axial positions to verify that all fields were <0.5 mT. The positions of these radial and axial locations in Table 1 indicate

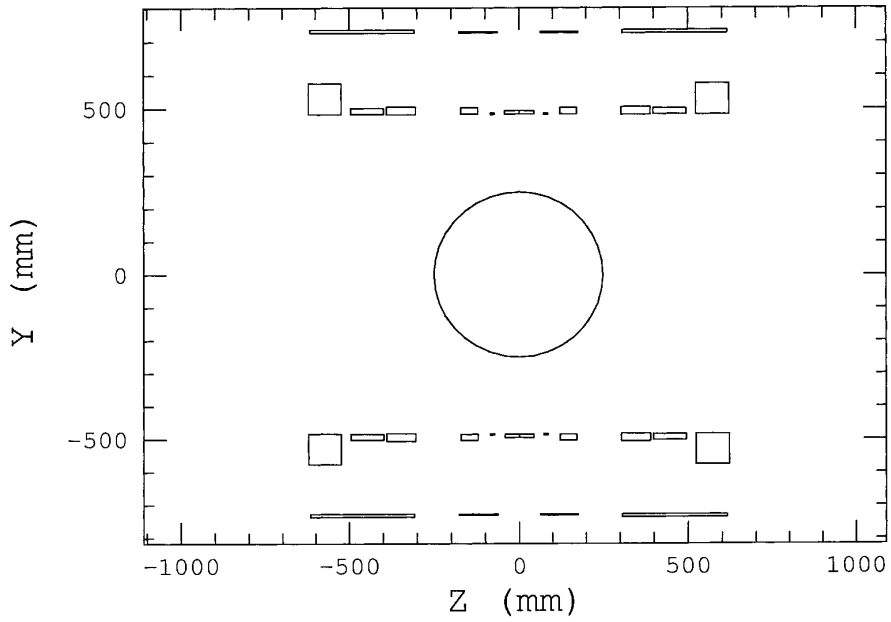

FIG. 2. Cross-section of the compact magnet pattern (design #1) relative to the dsv (circle).

small fringe fields. Table 2 gives the coil dimensions for design 1. Prior to construction, the number of turns in each coil is rounded and the SA routine re-run with axial position adjustment only. Inevitably, manufacturing tolerances lead to the presence of low order error terms when the magnet is constructed. These are usually easily nulled by passive or superconducting shim sets.

An important consideration in superconducting magnets is to ensure that the conductors are operating within acceptable limits of current density and submerged field

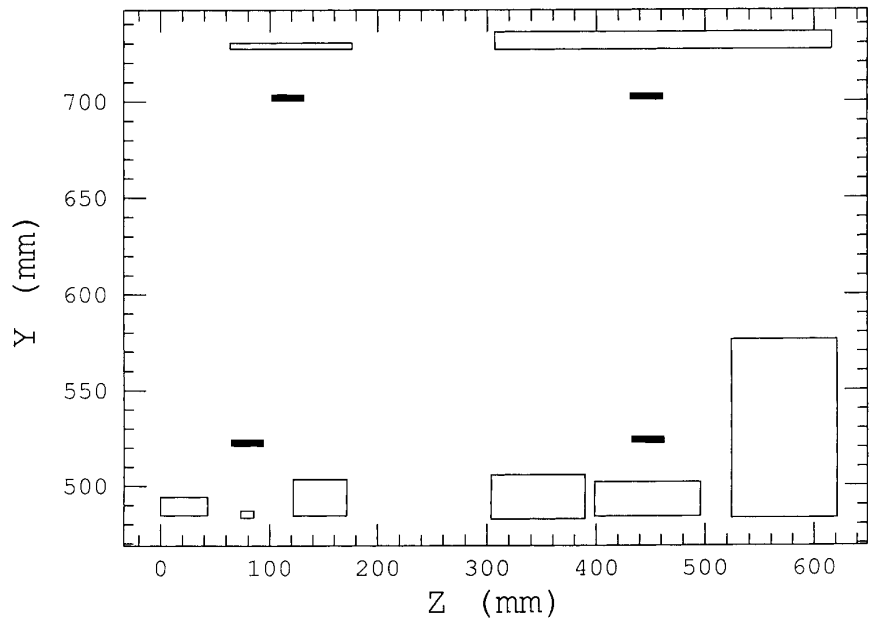

FIG. 3. An expanded view of the upper right-hand quadrant of Fig. 2; minus signs indicate coils wound counter to all others.

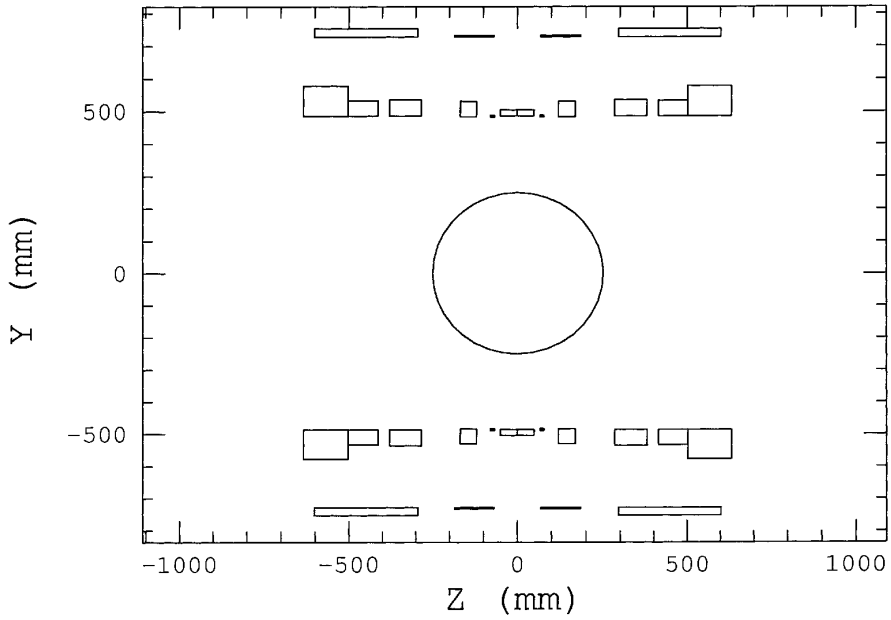

FIG. 4. An alternate design cross-section which used a smaller turns density (i.e., thicker wire). The dsv is again delimited by the central circle.

strengths (*23–25*). A disadvantage of using negative turns in the primary is that larger peak fields are generated in the coils than in all positive turn coil systems. Both of the designs considered here have peak fields of approximately 8 T with a transport current of about 250 A. Design 1 has a turns density in most coils of 100 cm^{-2} giving a current density of 2.5×10^8 A/m, while for Design 2 the current density was 1.0×10^8 A/m. For NbTi superconductor operating at 4.2 K these current densities are about 50% and 20% of the critical current density and the peak field is about 80% of the critical peak field. For Nb_3Sn conductor the margins are much improved (approximately twice as liberal).

In summary, we have shown that stochastic optimization produces novel, compact MRI magnet designs having excellent homogeneity and shielding. We have restricted ourselves to cylindrical, medical MRI systems in this work, but the method could be easily applied to magnets of other configurations.

TABLE 1

	Design 1	Design 2
Current for 1 T (A)	257	244.6
Length of conductor (km)	90.72	94.0
Homogeneity (45(40) cm dsv) (ppm)		
Peak-to-peak	16.4 (11.2)	9.1 (6.9)
Rms	4.2 (3.6)	2.1 (2.0)
Field harmonics (ppm)		
Z2	0.14 (0.1)	−0.8 (−0.6)
Z4	−1.2 (−0.8)	−0.6 (−0.4)
Z6	−0.99 (−0.05)	−0.3 (−0.2)
Z8	0.06 (0.02)	−0.2 (−0.09)
Z10	0.8 (0.24)	−5.0 (−1.5)
Z12	1.4 (0.34)	1 (−0.8)
Z14	−5.6 (−1.1)	−0.7 (−0.1)
Z16	−3.2 (−0.49)	1.3 (0.2)
Z18	−0.33 (−0.04)	3.0 (0.4)
Shielding 5 G contours (m)		
Axial	4.0	3.7
Radial	3.3	3.3

TABLE 2

Coil	Zed (mm)	Width (mm)	# Turns	Inner radius (mm)	t_d $(mm)^{-2}$
1	21.49	42.98	418.0	484.57	1.0
2	79.22	12.14	−45.17	483.42	1.0
3	146.55	49.86	941.37	484.55	1.0
4	346.6	85.96	1971.27	482.71	1.0
5	446.97	97.18	−1740.71	484.04	1.0
6	572.62	97.52	4534.84	483.21	0.5
7	119.99	112.81	−347.53	727.18	1.0
8	461.42	309.3	−2789.80	726.86	1.0

Note. Zed indicates the longitudinal position of the middle of each coil; *width* indicates the axial extent of each coil and t_d is the turns density.

ACKNOWLEDGMENT

We thank the Australian Research Council for support.

REFERENCES

1. M. W. Garrett, *J. Appl. Phys.* **22,** 1091 (1951).
2. M. W. Garrett, *J. Appl. Phys.* **38,** 2563 (1967).
3. H. Siebold, *IEEE Trans. Magn.* **26,** 841 (1990).
4. F. J. Davies, R. T. Elliott, and D. G. Hawkesworth, *IEEE Trans. Magn.* **27,** 1677 (1991).
5. A. K. Kalafala, *IEEE Trans. Magn.* **27,** 1696 (1991).
6. W. M. Schmidt, R. R. Huson, W. W. Mackay, and R. M. Rocha, *IEEE Trans. Magn.* **27,** 1681 (1991).
7. M. R. Thompson, R. W. Brown, and V. C. Srueastava, *IEEE Trans. Magn.* **30,** 108 (1994).
8. S. Crozier and D. M. Doddrell, *J. Magn. Reson.* **103,** 354 (1993).
9. S. Crozier, L. K. Forbes, and D. M. Doddrell, *J. Magn. Reson.* **107,** 126 (1994).
10. S. Crozier and D. M. Doddrell, *Magn. Reson. Imag.* **13,** 621 (1995).
11. M. L. Buszko, M. F. Kempka, E. Szezesniak, D. C. Wang, and E. R. Andrews, *J. Magn. Reson.* **112,** 207 (1996).
12. S. Kirkpatrick, C. D. Gelatt, and M. P. Vechhi, *Science* **220,** 671 (1983).
13. J. Simkin and C. W. Trowbridge, *IEEE Trans. Magn.* **28,** 1545 (1992).
14. G. Drago, A. Manella, M. Nerve, M. Repetto, and G. Secondo, *IEEE Trans. Magn.* **28,** 1541 (1992).
15. J. A. Vasconcelos, *IEEE Trans. Magn.* **32,** 1206 (1996).
16. D. Craik, ''Magnetism. Principles and Applications,'' Wiley, New York, 1995.
17. L. K. Forbes, S. Crozier, and D. M. Doddrell, in press, 1997.
18. L. K. Urankur, *IEEE Trans. Magn.* **18,** 1860 (1982).
19. S. Babric, Z. Andjelic, B. Krstajic, and S. Salon, *IEEE Trans. Magn.* **24,** 3162 (1988).
20. A. Corona, M. Marchesi, C. Martini, and S. Ridella, *ACM Trans. Math. Software* **13,** 262 (1987).
21. S. Crozier and D. M. Doddrell, U.S. Patent Application 08/576, 069 (1995).
22. M. Abramowitz and I. A. Stegun, ''Handbook of Mathematical Functions,'' National Bureau of Standards Applied Mathematics, 1972.
23. H. Brechna, ''Superconducting Magnet Systems,'' Springer-Verlag, Berlin/New York, 1973.
24. J. E. C. Williams, ''Superconducting and its Applications,'' Pion, London, 1970.
25. C. P. Poole, H. A. Farach, and R. J. Creswick, ''Superconductivity,'' Academic Press, San Diego, 1995.